Electronic Supplementary Information

Subnanometric Pt clusters supported on MgO-incorporated porous carbon as an efficient metal-base bifunctional catalyst for reductive heterocyclization reactions

Yaping Song,[a#] Ruifang Xue,[a#] Li Wang,[a] Nan Li,[a] Zhijun Fang,[a] Yanghe Fu,[a, b] De-Li Chen,[a, b]* Weidong Zhu,[a, b]* and Fumin Zhang[a, b]*

[a]Key Laboratory of the Ministry of Education for Advanced Catalysis Materials, Institute of Physical Chemistry, Zhejiang Normal University, Jinhua 321004, People's Republic of China

[b]Zhejiang Engineering Laboratory for Green Syntheses and Applications of Fluorine-Containing Specialty Chemicals, Institute of Advanced Fluorine-Containing Materials, Zhejiang Normal University, Jinhua 321004, People's Republic of China

[#]These authors contributed equally to this work

*Corresponding Authors:

De-Li Chen: chendl@zjnu.cn;

Weidong Zhu: weidongzhu@zjnu.cn;

Fumin Zhang: zhangfumin@zjnu.edu.cn

Table S1 Pt and Mg loadings as well as the textural properties of various catalysts investigated

Sample	$S_{BET}{}^a$ (m²/g)	$V_{total}{}^b$ (cm³/g)	Pt loading[c] (wt%)	Mg loading[c] (wt%)
Pt/MgO@C	614.4	0.82	0.078	20.57
Pt/MgO	57.6	0.36	0.075	-
Pt/C	851.9	0.49	0.079	-
Pt/Al$_2$O$_3$	15.6	0.13	0.095	-
Pt/SiO$_2$	238.6	1.52	0.080	-
Pt/C + MgO	532.5	0.46	0.079	-

[a]By BET method. [b]By t−plot method. [c]By ICP−AES analysis.

Table S2 Catalytic performance of Pt/MgO@C for the reductive heterocyclization of 2-nitrobenzaldehyde with different solvent

Entry	Solvent	Time (h)	Con. (%)	Sel. (%)	TOF^a (h^{-1})
1	Toluene	6	≥99	98.5	240
2	MeOH	8	≥99	95.7	210
3	THF	6	11	83.9	18.3
4^b	H_2O	10	22	85.9	22
5	EtOH	5.5	≥99	94.8	266.7
6	EtOH/H_2O (V/V=1:1)	3	≥99	91.9	285

Reaction conditions: catalyst (50 mg, 0.1 mol%), 2-nitrobenzaldehyde (0.2 mmol), solvent (3 mL), 303 K, H_2 (1 bar in balloon). ^{a}TOF values were calculated as the number of moles of 2,1-benzisoxazole produced by per mole of Pt sites per hour. ^{b}2-Nitrobenzaldehyde is partially soluble in water.

Table S3 Comparison of the performance of the reductive heterocyclization of 2-nitrobenzaldehyde in the literature

Entry	Catalyst	Solvent	Temp. (K)	Time (h)	Yield (%)	Ref.
1	Pt/MgO@C	Toluene	303	6	98.5	This work
2	BNP (2 equiv)/In (5 equiv)	MeOH/H$_2$O (V/V=1:2)	323	0.17	93	[S1]
3	In (3 equiv)/I$_2$ (0.8 equiv)	MeOH	323	1.5	87	[S2]
4	SnCl$_2$·2H$_2$O	EtOAc/MeOH (V/V=1:1)	298	20	86	[S3]
5	Ir60 : G6/SiO$_2$	Toluene	303	1	41	[S4]
6	Pt/MgO	Toluene	303	1	94	[S5]
7	Pt/c-C	MeOH	303	3	92	[S6]

Reference

[S1]   B. H. Kim, Y. Jin, Y. M. Jun, R. B. Han, W. Baik and B. M. Lee, *Tetrahedron Lett.*, 2000, **41**, 2137−2140.

[S2]   R. B. Han, K. I. Son, G. H. Ahn, Y. M. Jun, B. M. Lee, Y. Park and B. H. Kim, *Tetrahedron Lett.*, 2006, **47**, 7295−7299.

[S3]   J. Chauhan and S. Fletcher, *Tetrahedron Lett.*, 2012, **53**, 4951−4954.

[S4]   T. Higaki, H. Kitazawa, S. Yamazoe and T. Tsukuda, *Nanoscale*, 2016, **8**, 11371−11374.

[S5]   L. Marti, L. M. Sanchez, M. J. Climent, A. Corma, S. Iborra, G. P. Romanelli and P. Concepcion, *ACS Catal.*, 2017, **7**, 8255−8262.

[S6]   Y. Y. Wu, Y. F. Zhao, H. Wang, F. T. Zhang, R. P. Li, J. F. Xiang, Z. P. Wang, B. X. Han and Z. M. Liu, *Green Chem.*, 2020, **22**, 3820−3826.
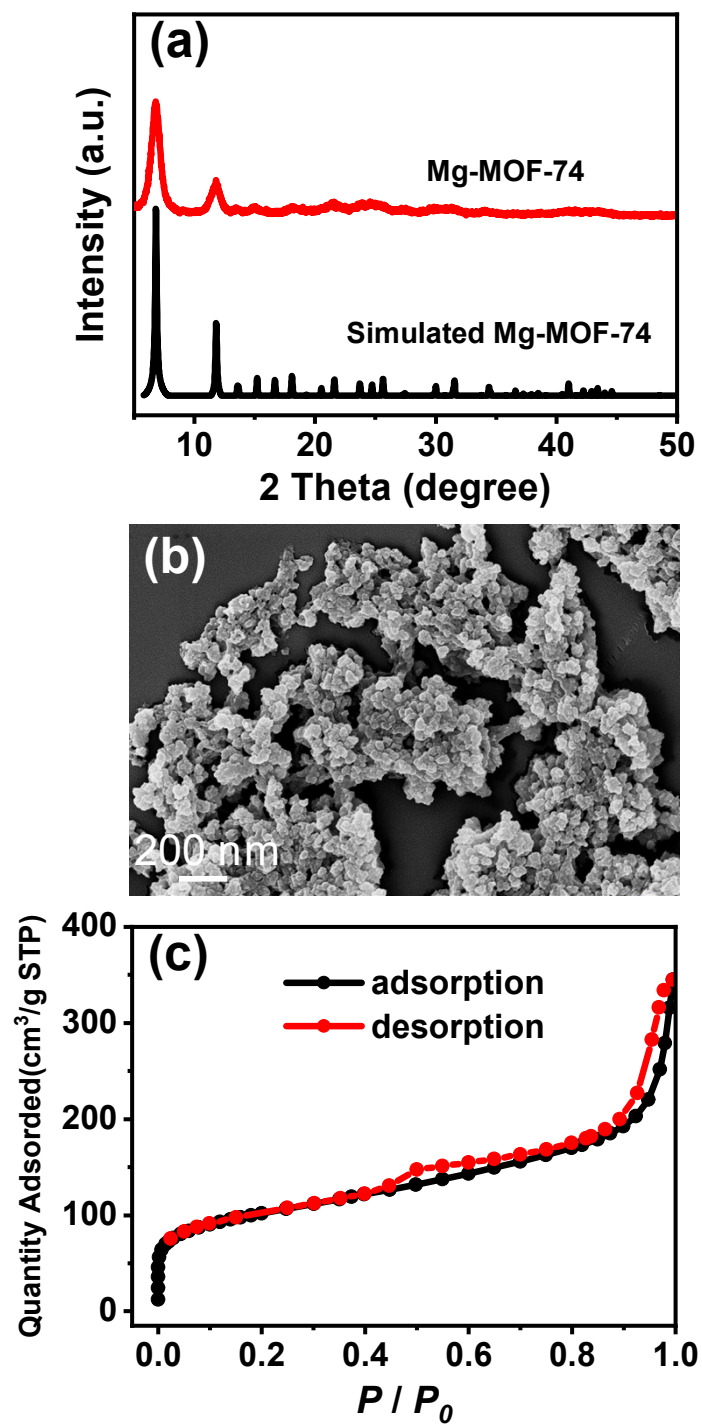
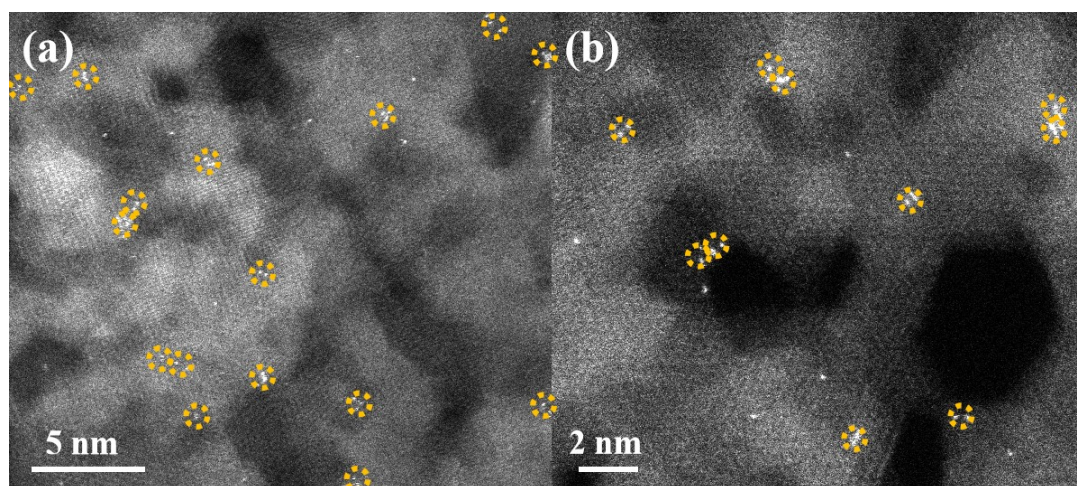**Figure S1** XRD pattern (a), SEM (b), and N$_2$ adsorption–desorption isotherms (c) of Mg-MOF-74.

Figure S2 Aberration-corrected HAADF−STEM images of Pt/MgO@C catalyst.
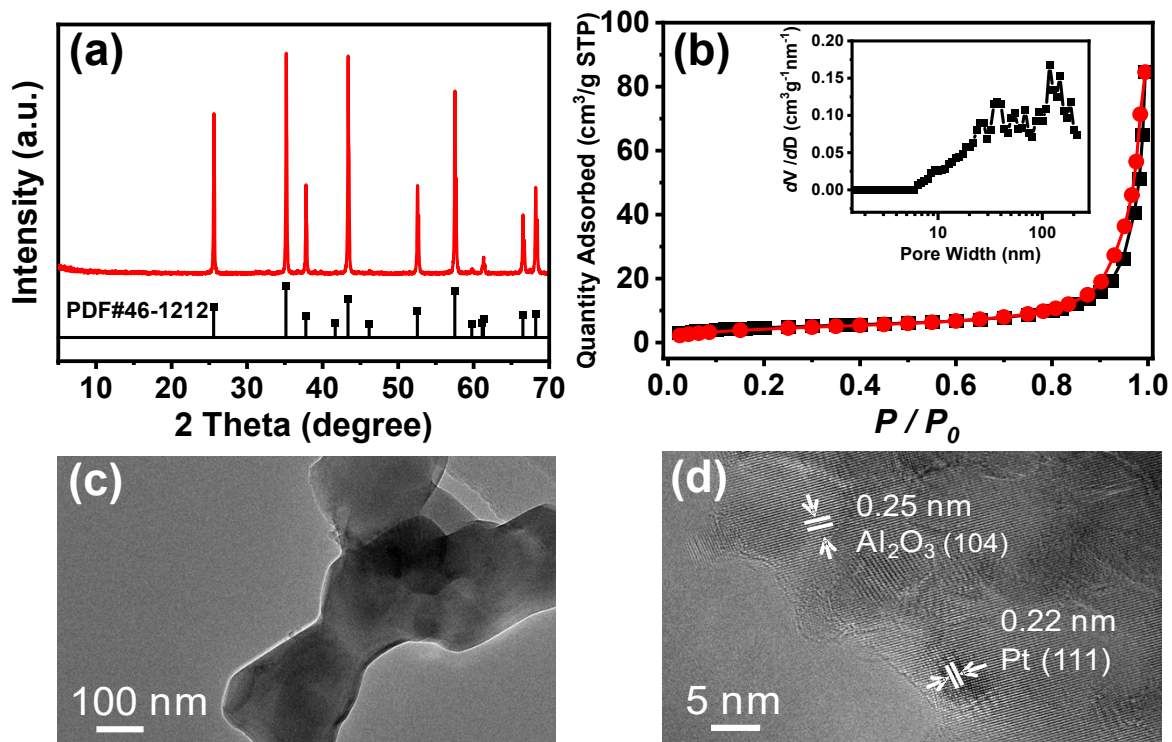
Figure S3 XRD pattern (a), N_2 adsorption−desorption isotherms and the corresponding pore size distribution (inset) (b), TEM (c), and HRTEM images (d) of the Pt/Al_2O_3 catalyst.
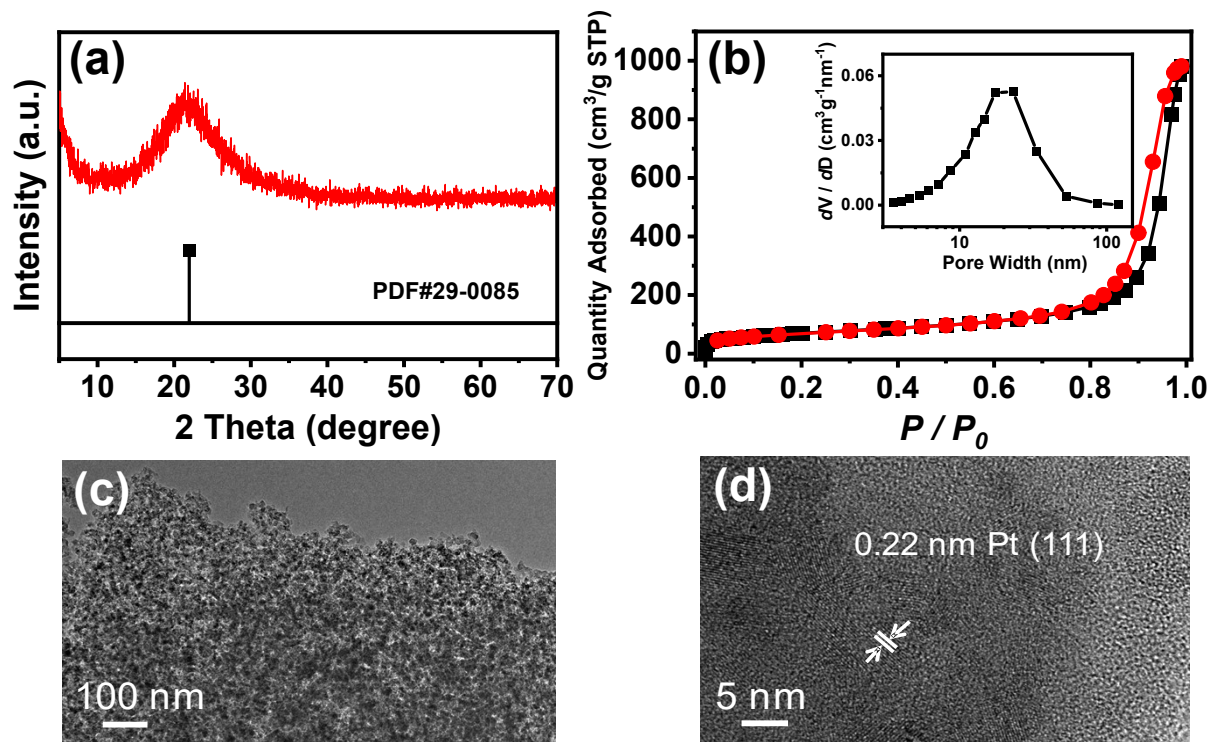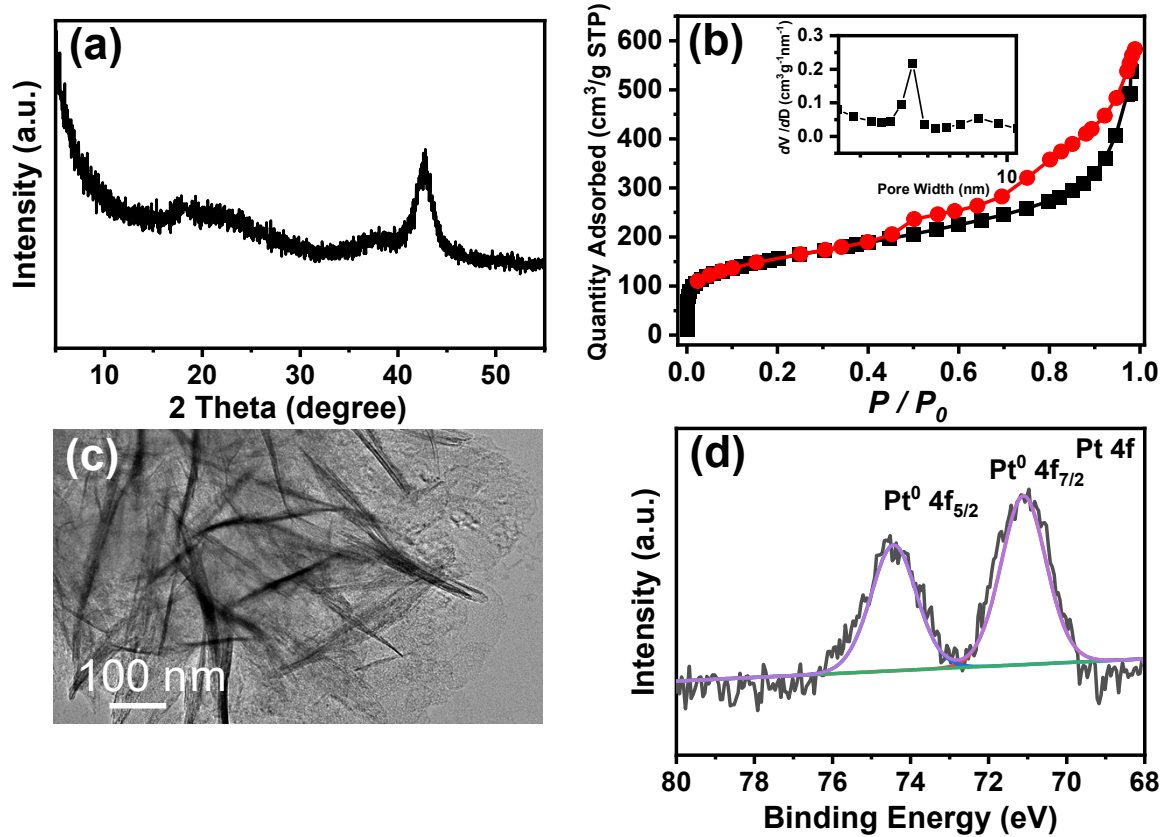
**Figure S4** XRD pattern (a), N_2 adsorption−desorption isotherms and the corresponding pore size distribution (inset) (b), TEM (c), and HRTEM images (d) of the Pt/SiO_2 catalyst.
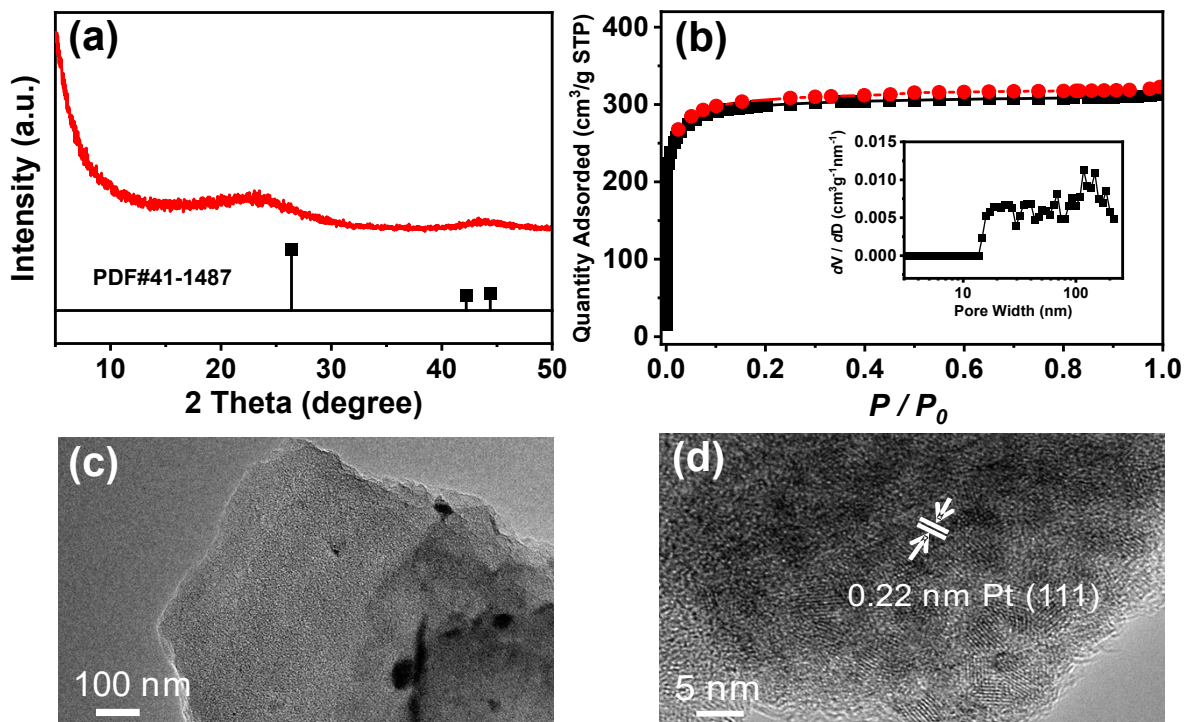
Figure S5 XRD pattern (a), N_2 adsorption−desorption isotherms and the corresponding pore size distribution (inset) (b), TEM (c), and HRTEM images (d) of the Pt/C catalyst.
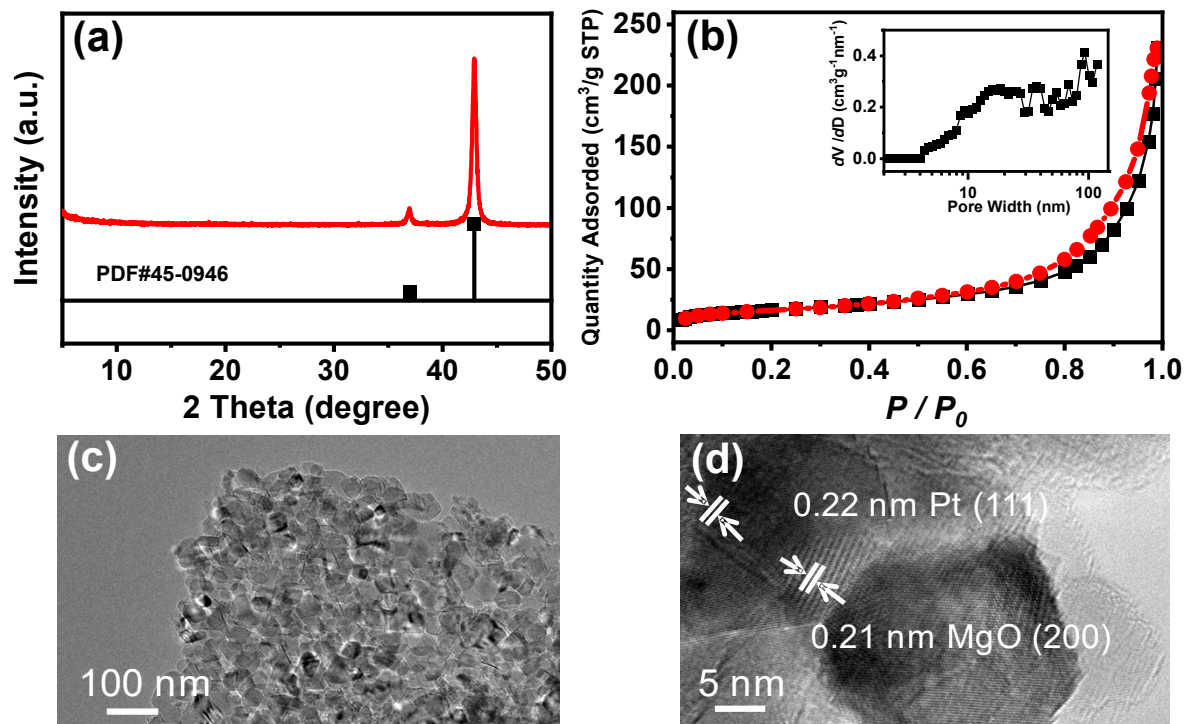
Figure S6 XRD pattern (a), N_2 adsorption−desorption isotherms and the corresponding pore size distribution (inset) (b), TEM (c), and HRTEM images (d) of the Pt/MgO catalyst.

Figure S7 XRD pattern (a), N_2 adsorption−desorption isotherms and the corresponding pore size distribution (inset) (b), TEM (c), and Pt 4f XPS spectra (d) of the spent Pt/MgO@C catalyst.
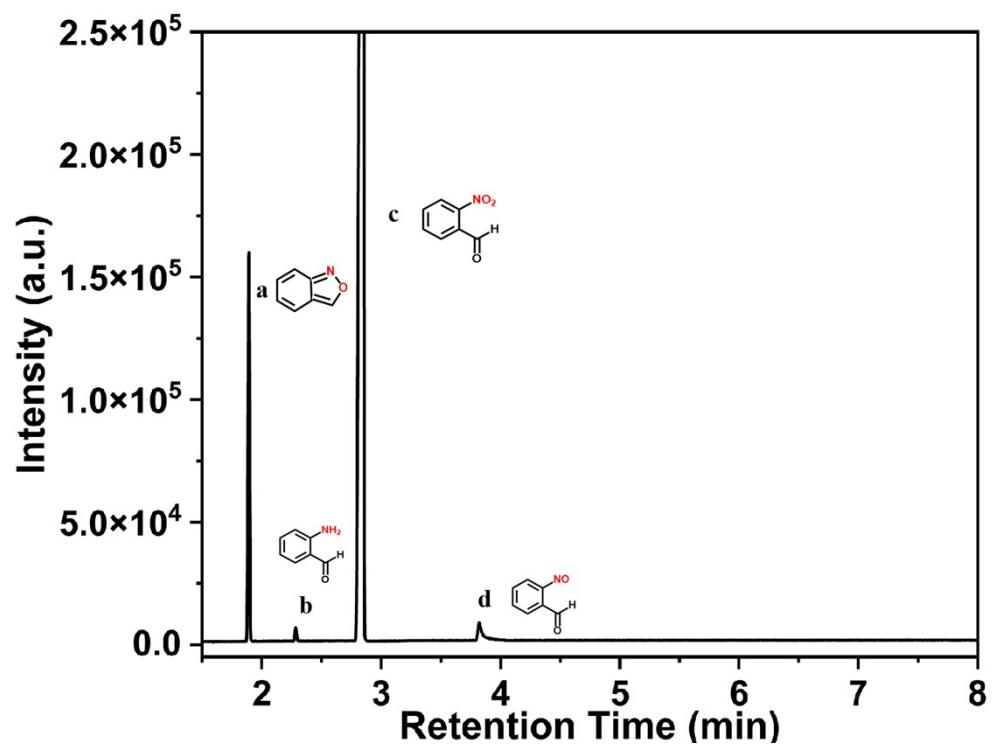
Figure S8 GC−MS spectrum of reactant, intermediate, and products. Reaction conditions: Pt/MgO@C (50 mg), 2-nitrobenzaldehyde (0.2 mmol), toluene (3 mL), 273 K, 0.5 h, H_2 (1 bar in balloon).
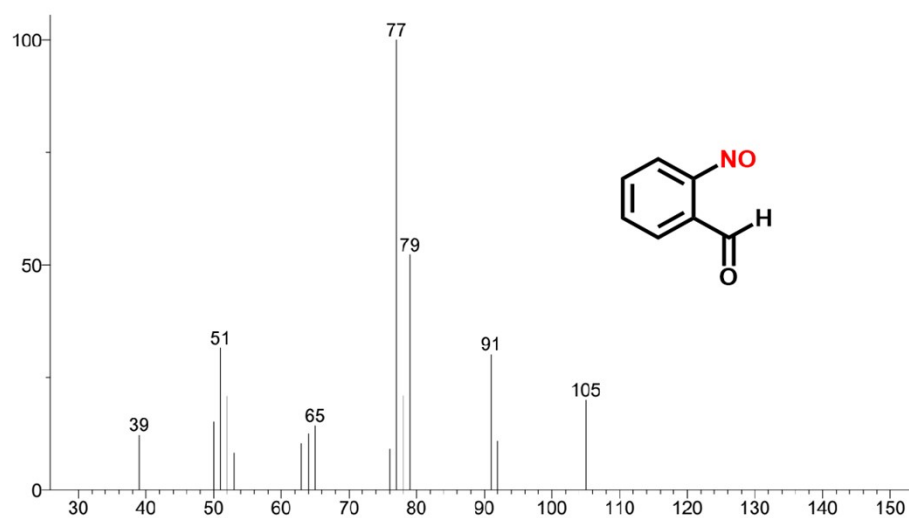
Figure S9 GC−MS spectrum of nitroso compounds. Reaction conditions: Pt/MgO@C (50 mg), 2-nitrobenzaldehyde (0.2 mmol), toluene (3 mL), 273 K, 0.5 h, H_2 (1 bar in balloon).

E_{ads} = -1.15 eV E_{ads} = -0.71 eV E_{ads} = -0.87 eV
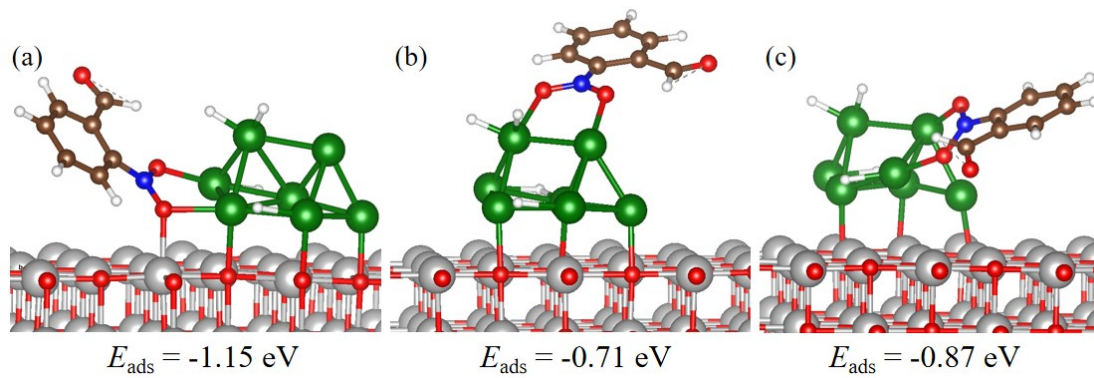
Figure S10 Stable configurations for the adsorption of 2-nitrobenzaldehyde on Pt$_7$/MgO(100)

as well as their adsorption energies.
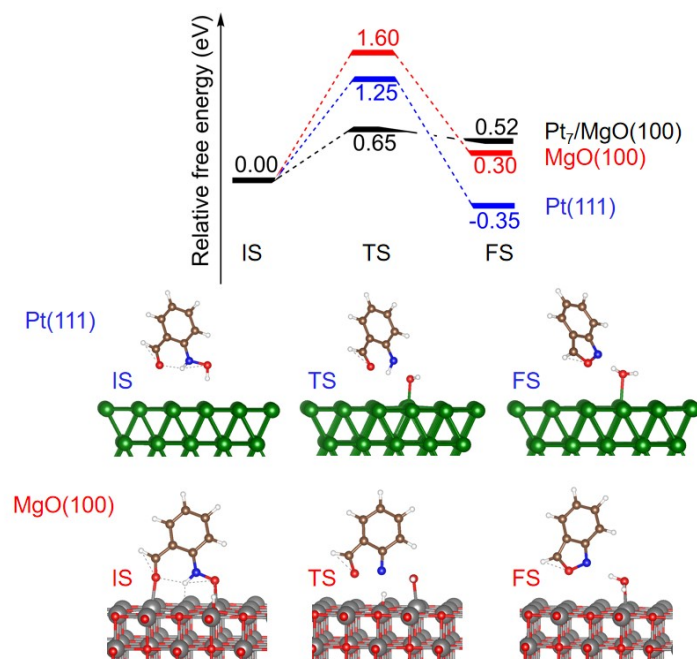
Figure S11 Comparison of reaction pathways for the heterocyclization reaction of hydroxylamine to 2,1-benzisoxazole on $Pt_7/MgO(100)$, $MgO(100)$, and $Pt(111)$ surfaces.

Analytical data of the products

2,1-Benzisoxazole [S7]
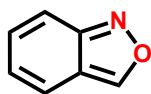
A yellow oil. ^{1}H NMR (600 MHz, CDCl$_3$) δ 9.10 (s, 1H), 7.58 (d, J = 9.1 Hz, 1H), 7.56 (d, J = 8.8 Hz, 1H), 7.26 (dd, J = 9.1, 6.3 Hz, 1H), 6.95 (dd, J = 8.8, 6.4 Hz, 1H). ^{13}C NMR (151 MHz, CDCl$_3$) δ 155.95, 154.50, 130.81, 124.28, 119.60, 118.07, 114.80.

3-Methyl-2,1-benzisoxazole [S7]
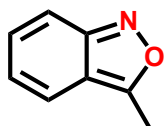
A yellow oil. ^{1}H NMR (600 MHz, CDCl$_3$) δ 7.51 (d, J = 8.7 Hz, 1H), 7.43 (d, J = 9.1 Hz, 1H), 7.27 (dd, J = 9.1, 6.3 Hz, 1H), 6.92 (dd, J = 8.7, 6.4 Hz, 1H), 2.79 (s, 3H). ^{13}C NMR (151 MHz, CDCl$_3$) δ 165.74, 157.14, 130.86, 122.85, 119.93, 115.71, 114.94, 12.04.

5-Chloro-2,1-benzisoxazole [S8]
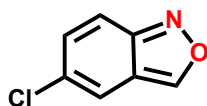
A yellow solid. ^{1}H NMR (600 MHz, CDCl$_3$) δ 9.11 (s, 1H), 7.61 (d, J = 9.4 Hz, 1H), 7.58 (s, 1H), 7.25 (dd, J = 9.4, 1.6 Hz, 1H). ^{13}C NMR (151 MHz, CDCl$_3$) δ 154.70, 154.17, 132.89, 130.34, 118.54, 117.91, 116.90.

4-Chloro-2,1-benzisoxazole [S9]
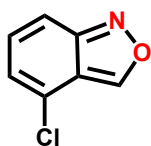
A green solid. ^{1}H NMR (600 MHz, CDCl$_3$) δ 9.19 (s, 1H), 7.52 (d, J = 9.0 Hz, 1H), 7.21 (t, J = 9.0 Hz, 1H), 6.99 (d, J = 6.9 Hz, 1H). ^{13}C NMR (151 MHz, CDCl$_3$) δ 156.68, 154.91, 131.22, 125.38, 123.38, 119.53, 113.90.

[1,3]Dioxolo[4,5-f]-2,1-benzisoxazole [S7]
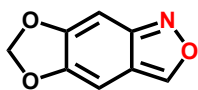
A yellow solid. ^{1}H NMR (600 MHz, CDCl$_3$) δ 8.77 (s, 1H), 6.78 (s, 1H), 6.66 (s, 1H), 5.98 (s, 2H). ^{13}C NMR (151 MHz, CDCl$_3$) δ 155.54, 153.00, 152.16, 147.76, 115.37, 101.90, 92.16, 89.68.
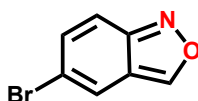
6-Methyl-2,1-benzisoxazole [S7]
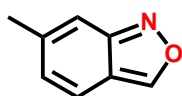
An orange oil. ^{1}H NMR (600 MHz, CDCl$_3$) δ 9.02 (s, 1H), 7.44 (d, J = 8.9 Hz, 1H), 7.34 (s, 1H), 6.84 (d, J = 8.1 Hz, 1H), 2.39 (s, 3H). ^{13}C NMR (151 MHz, CDCl$_3$) δ 156.85, 153.97, 141.35, 127.98, 119.09, 117.14, 112.51, 22.50.

6-Chloro-2,1-benzisoxazole [S7]
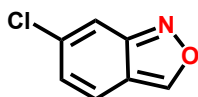
A pale-yellow solid. ^{1}H NMR (600 MHz, CDCl$_3$) δ 9.11 (s, 1H), 7.62 (s, 1H), 7.52 (d, J = 9.2 Hz, 1H), 6.95 (dd, J = 9.2, 1.6 Hz, 1H). ^{13}C NMR (151 MHz, CDCl$_3$) δ 156.28, 155.22, 137.33, 126.72, 121.12, 116.79, 113.78.

5-Bromo-2,1-benzisoxazole [S10]

An orange solid. ^{1}H NMR (600 MHz, CDCl$_3$) δ 9.12 (d, J = 1.1 Hz, 1H), 7.77 (d, J = 2.9 Hz, 1H), 7.54 (ddd, J = 9.5, 4.5, 0.9 Hz, 1H), 7.35 (ddd, J = 9.3, 4.9, 1.6 Hz, 1H). ^{13}C NMR (151 MHz, CDCl$_3$) δ 154.57, 154.01, 134.93, 121.53, 119.31, 118.21, 116.88.

4-Bromo-2,1-benzisoxazole [S8]
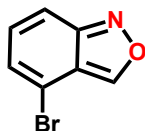
A pale-yellow solid. ^{1}H NMR (600 MHz, CDCl$_3$) δ 9.08 (s, 1H), 7.52-7.50 (m, 1H), 7.13-7.07 (m, 2H). ^{13}C NMR (151 MHz, CDCl$_3$) δ 156.27, 156.23, 131.54, 126.93, 121.05, 114.41, 112.63.

5-Methoxy-2,1-benzisoxazole [S11]
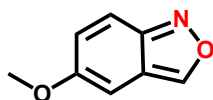
A yellow oil. ^{1}H NMR (600 MHz, CDCl$_3$) δ 8.91 (s, 1H), 7.51 (d, J = 9.6 Hz, 1H), 7.01 (dd, J = 9.6, 1.6 Hz, 1H), 6.60 (s, 1H), 3.80 (s, 3H). ^{13}C NMR (151 MHz, CDCl$_3$) δ 156.28, 154.47, 152.37, 128.27, 118.39, 116.62, 92.86, 55.44.
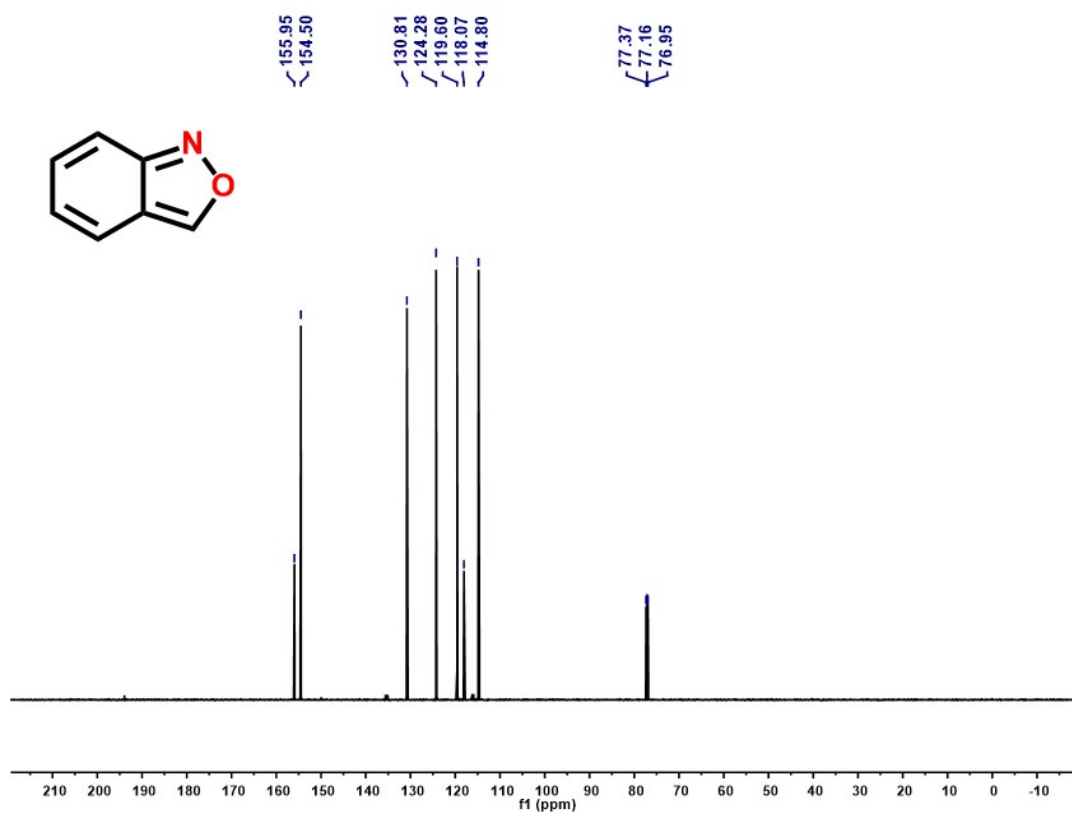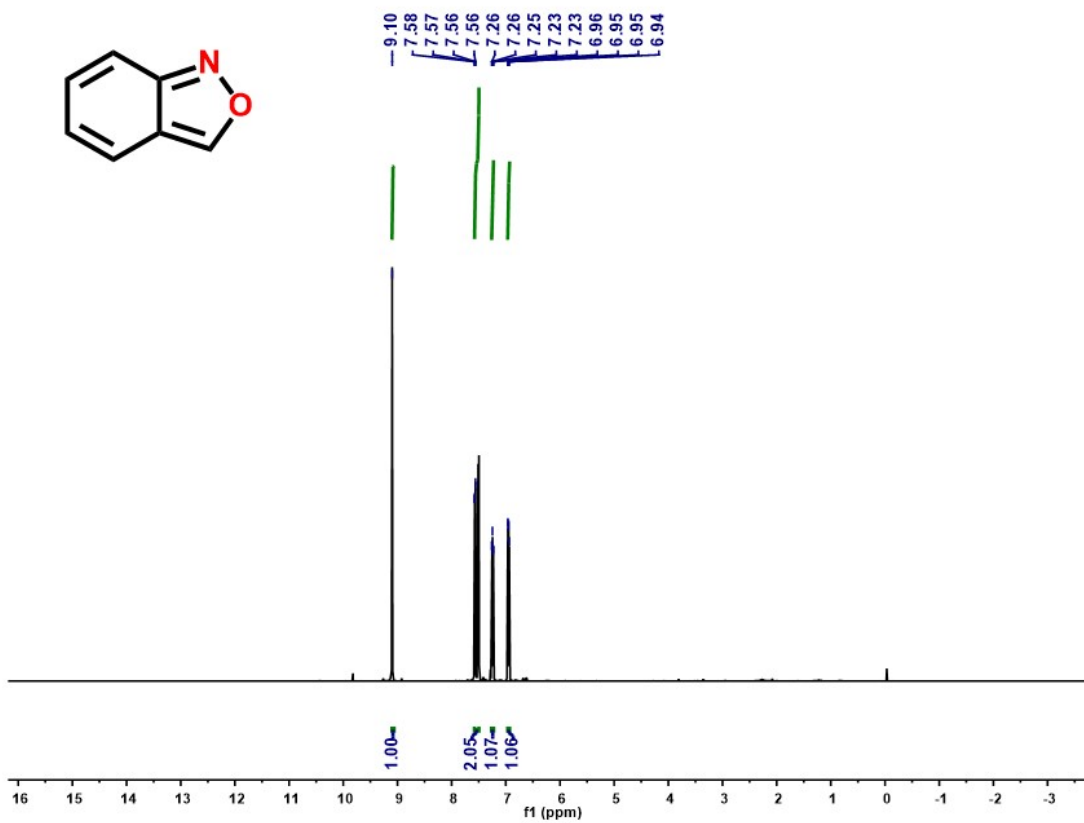
Figure S12 ^{1}H and ^{13}C NMR spectra for 2,1-benzisoxazole.
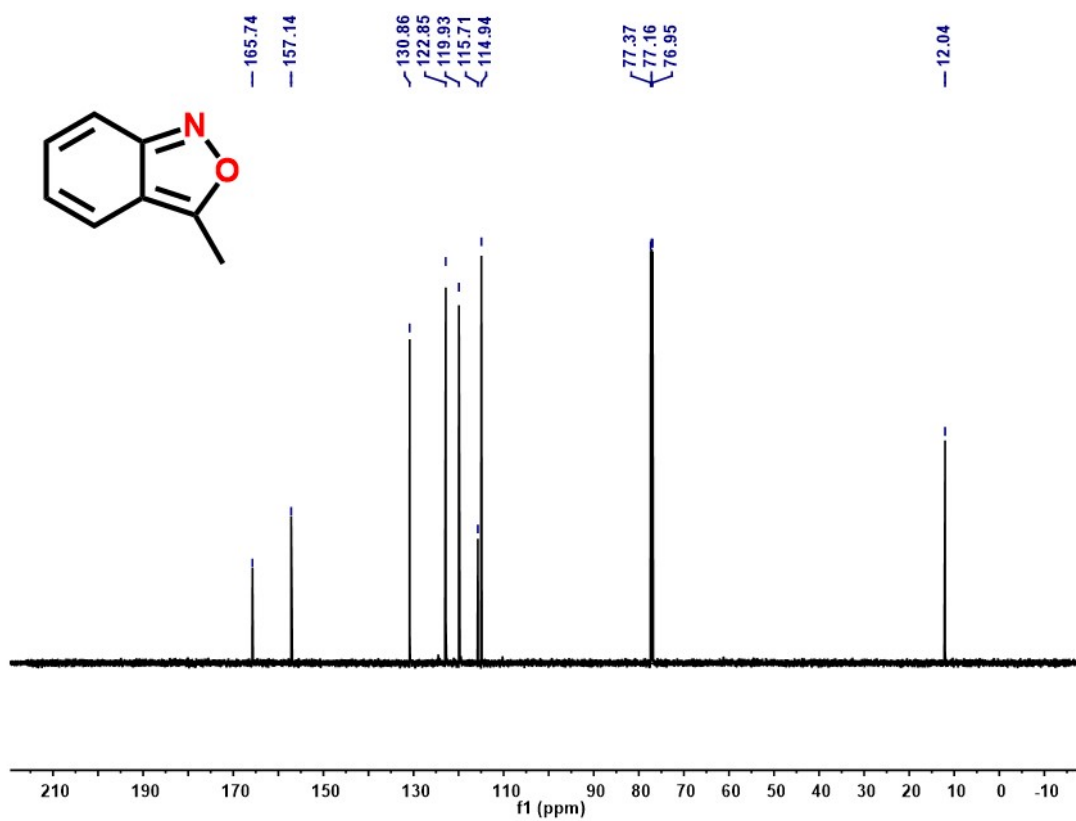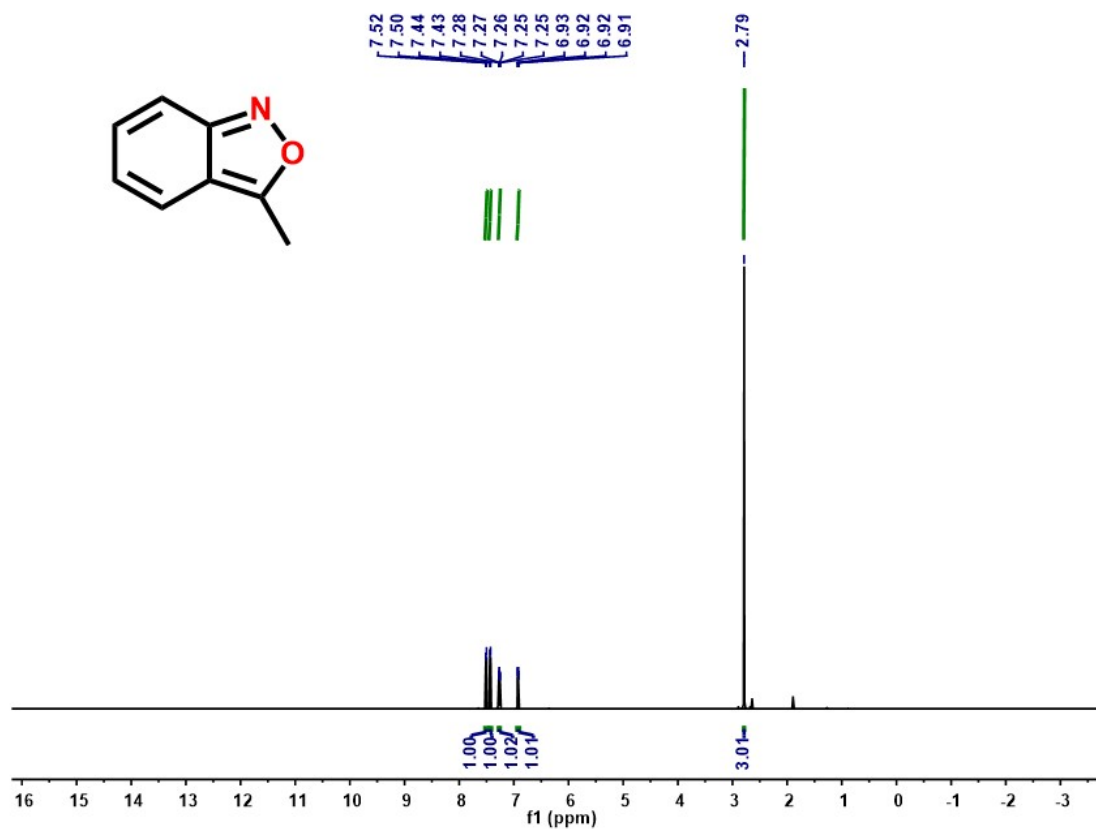
Figure S13 ^{1}H and ^{13}C NMR spectra for 3-methyl-2,1-benzisoxazole.
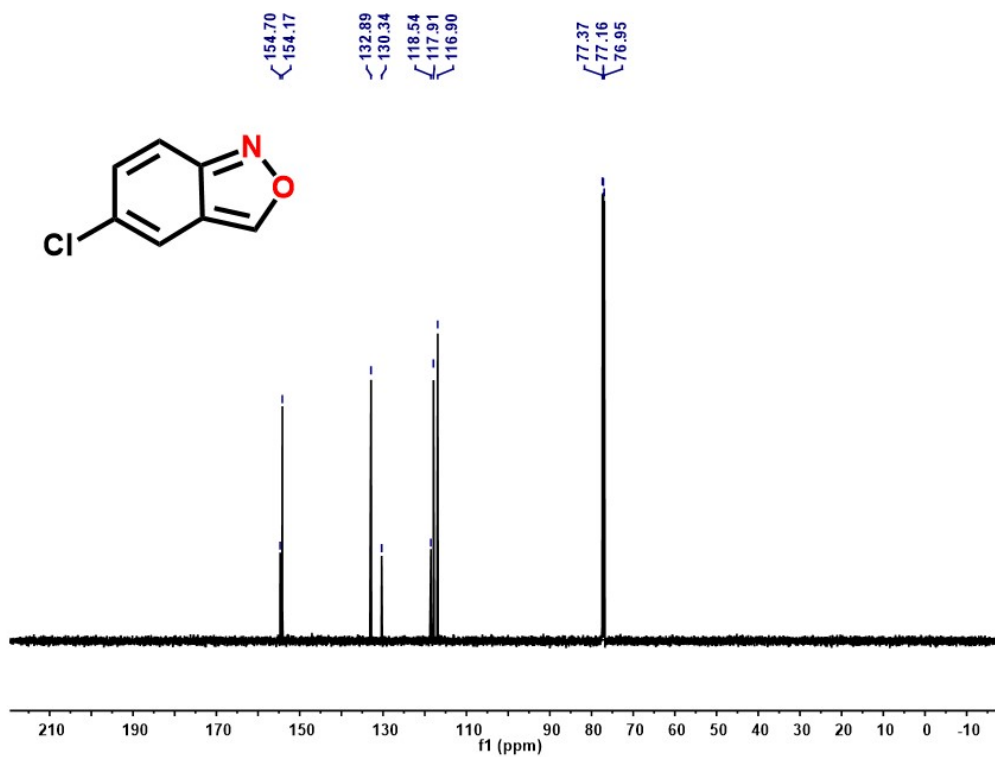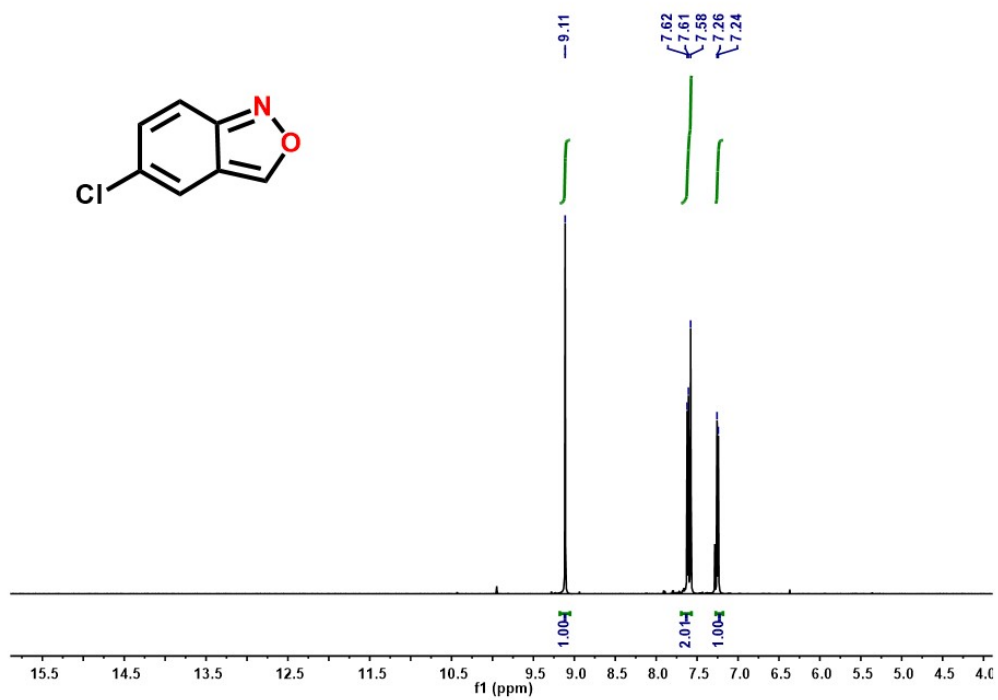
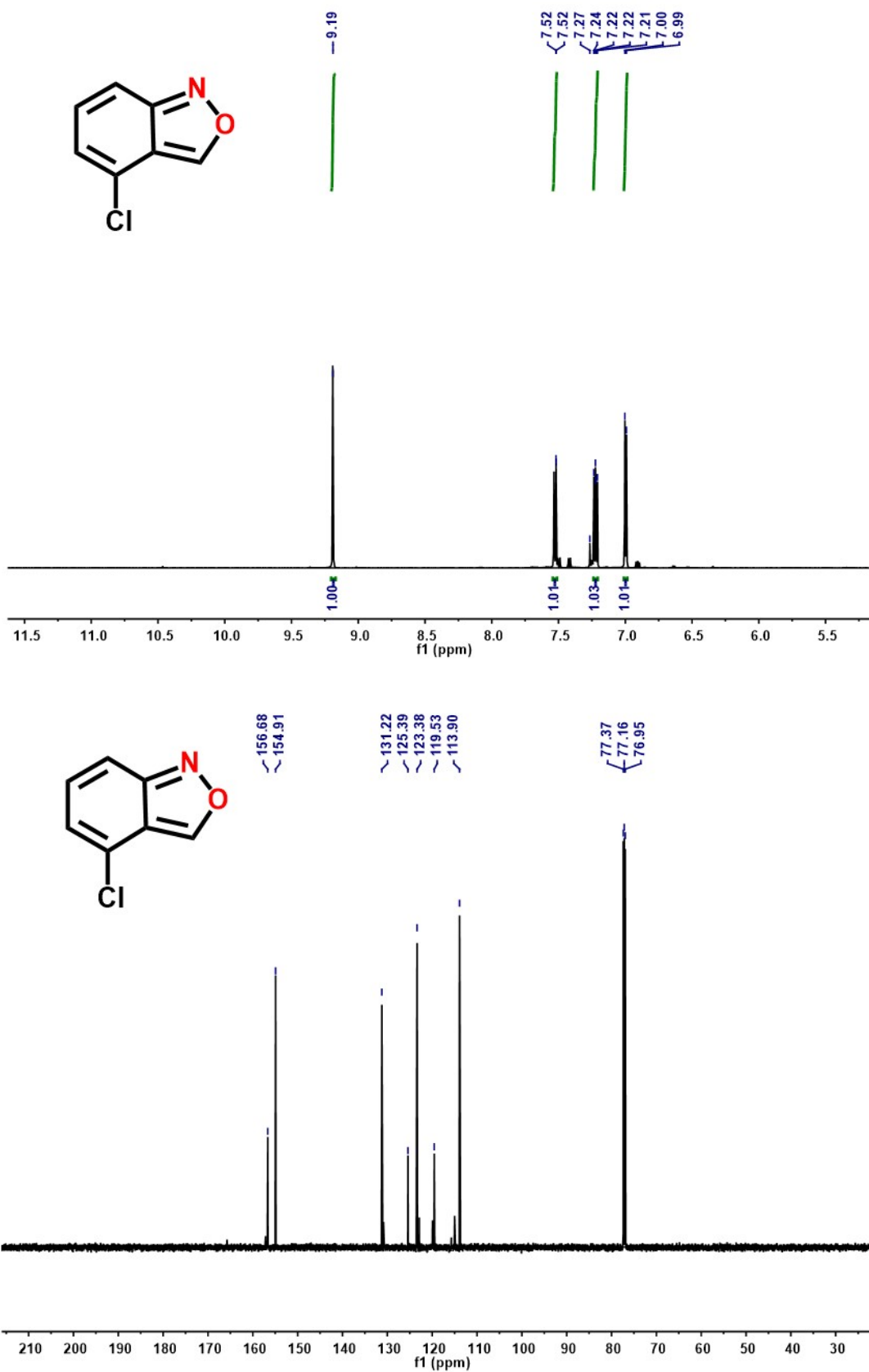**Figure S14** ^{1}H and ^{13}C NMR spectra for 5-chloro-2,1-benzisoxazole.

Figure S15 ¹H and ¹³C NMR spectra for 4-chloro-2,1-benzisoxazole.
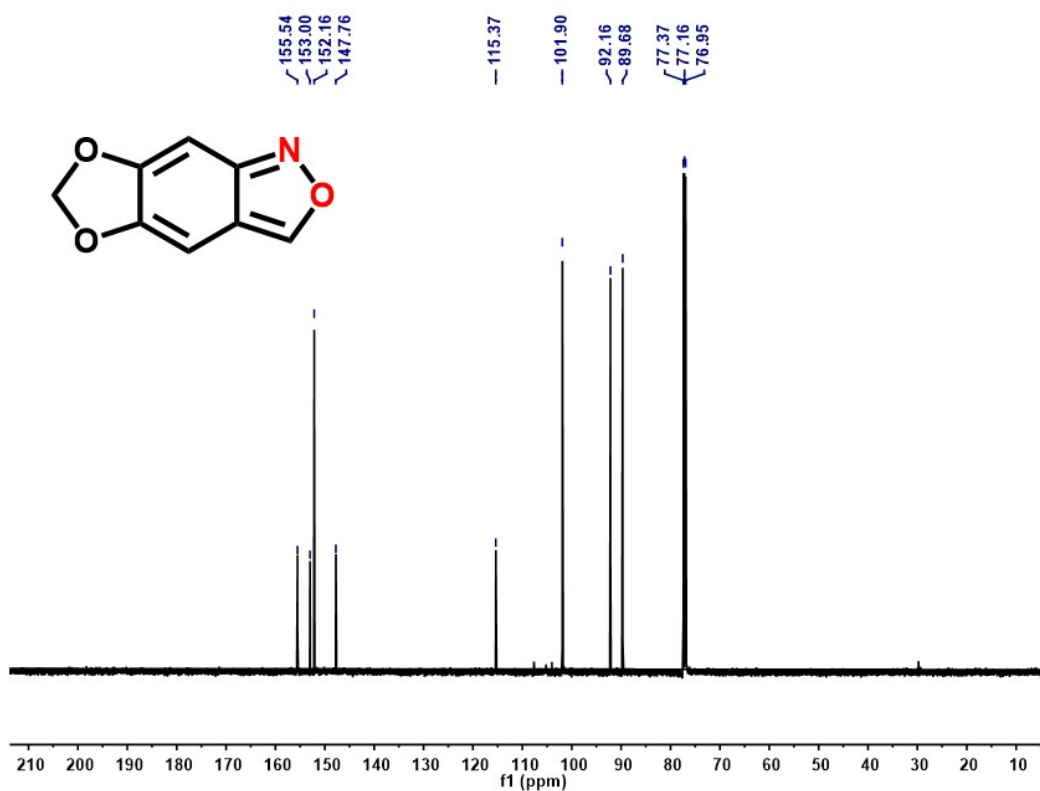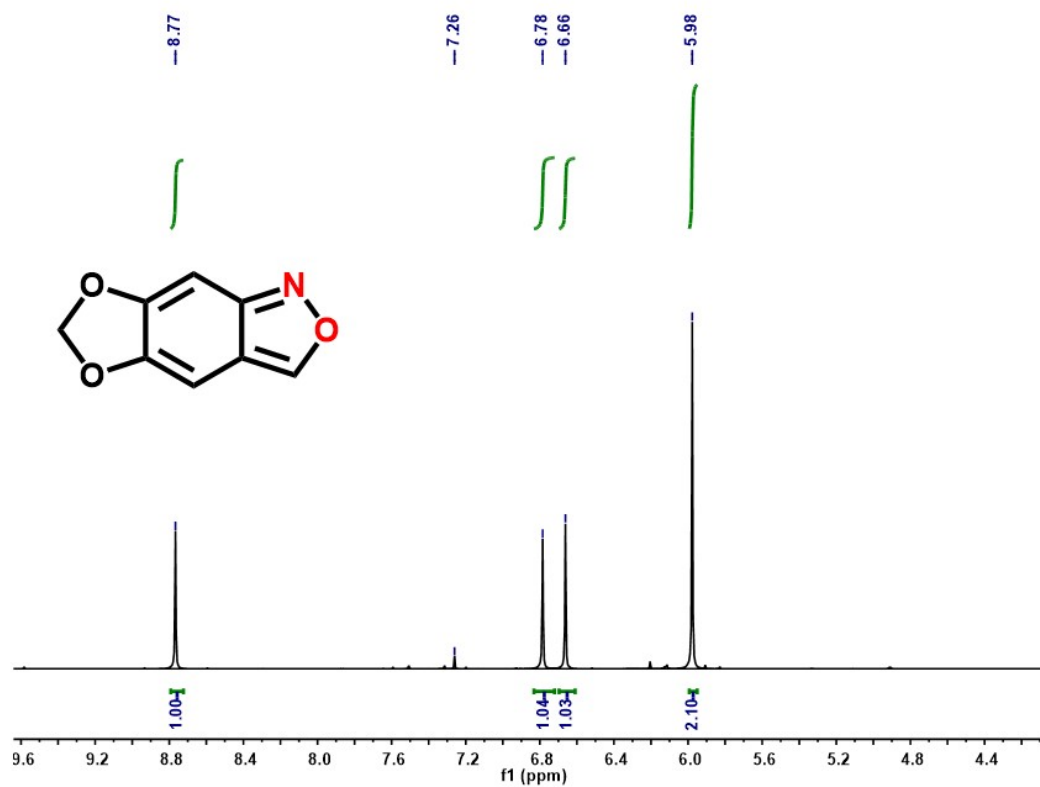
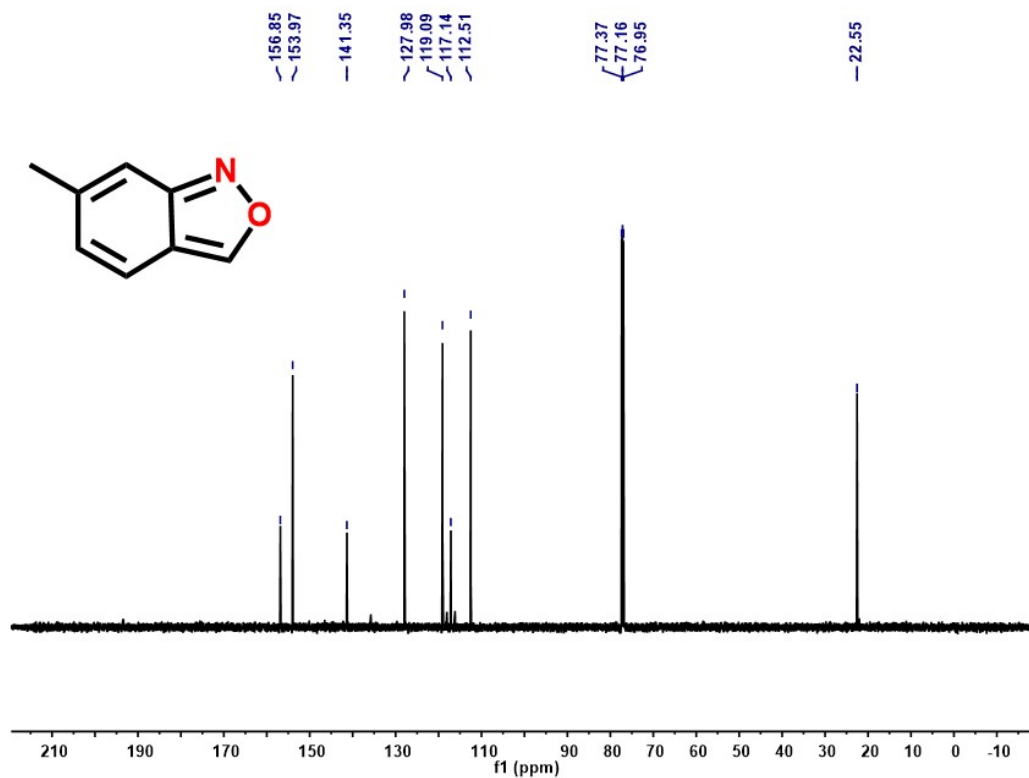**Figure S16** ^{1}H and ^{13}C NMR spectra for [1,3]dioxolo[4,5-f]-2,1-benzisoxazole.
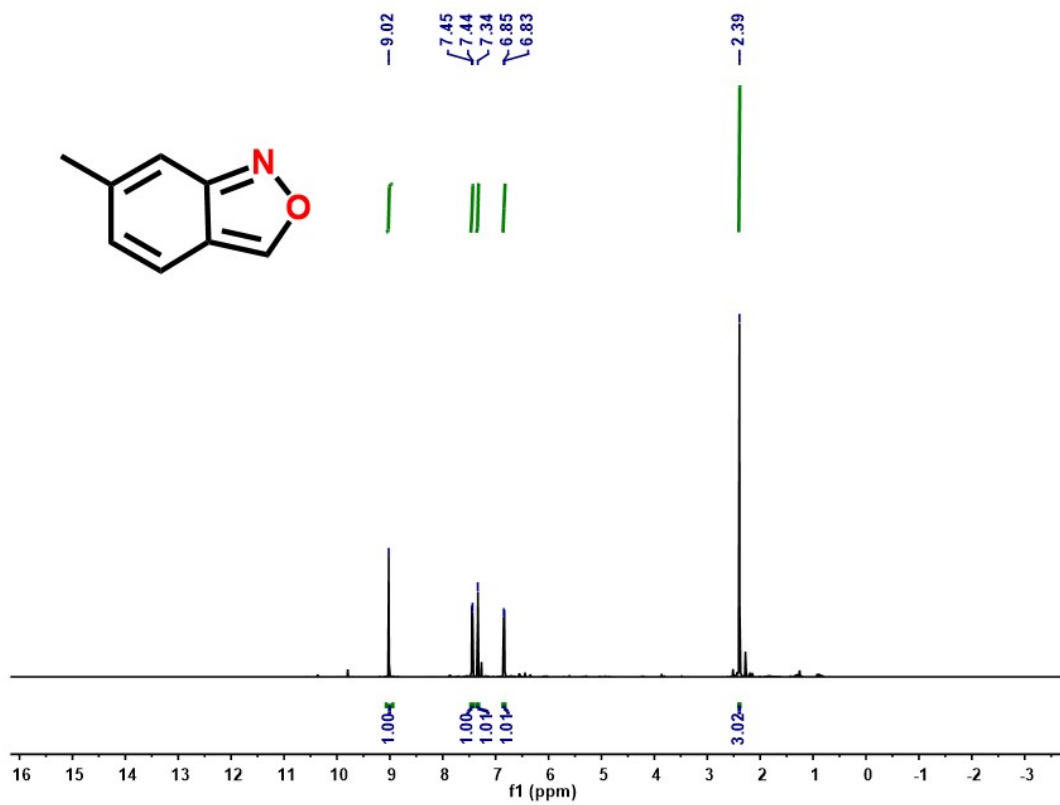
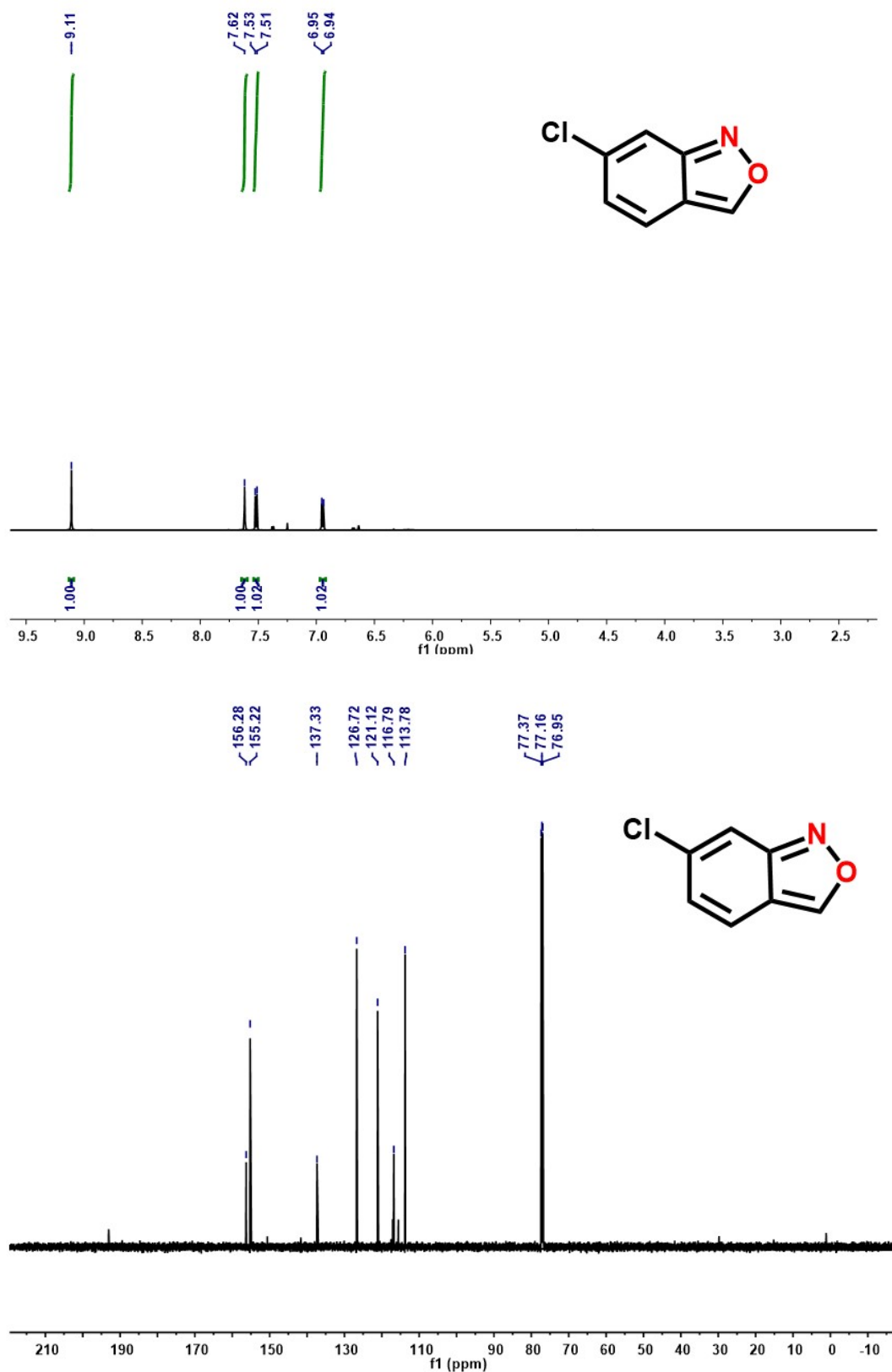**Figure S17** ^{1}H and ^{13}C NMR spectra for 6-methyl-2,1-benzisoxazole.

Figure S18 ^{1}H and ^{13}C NMR spectra for 6-chloro-2,1-benzisoxazole.
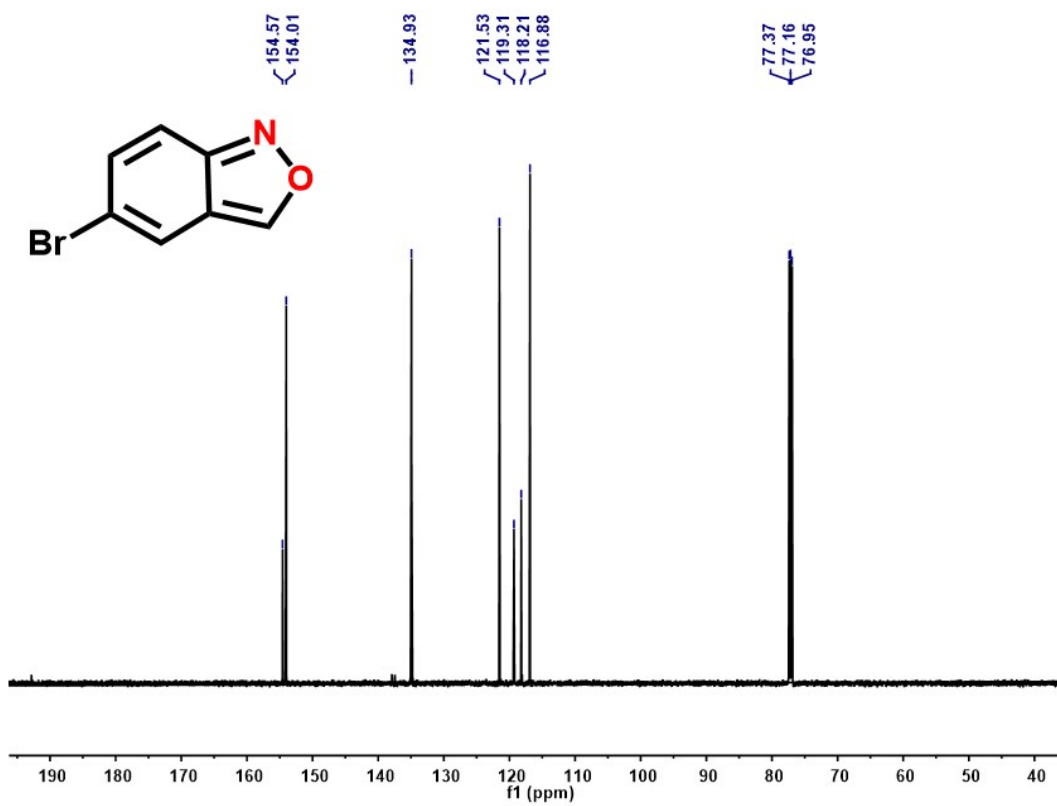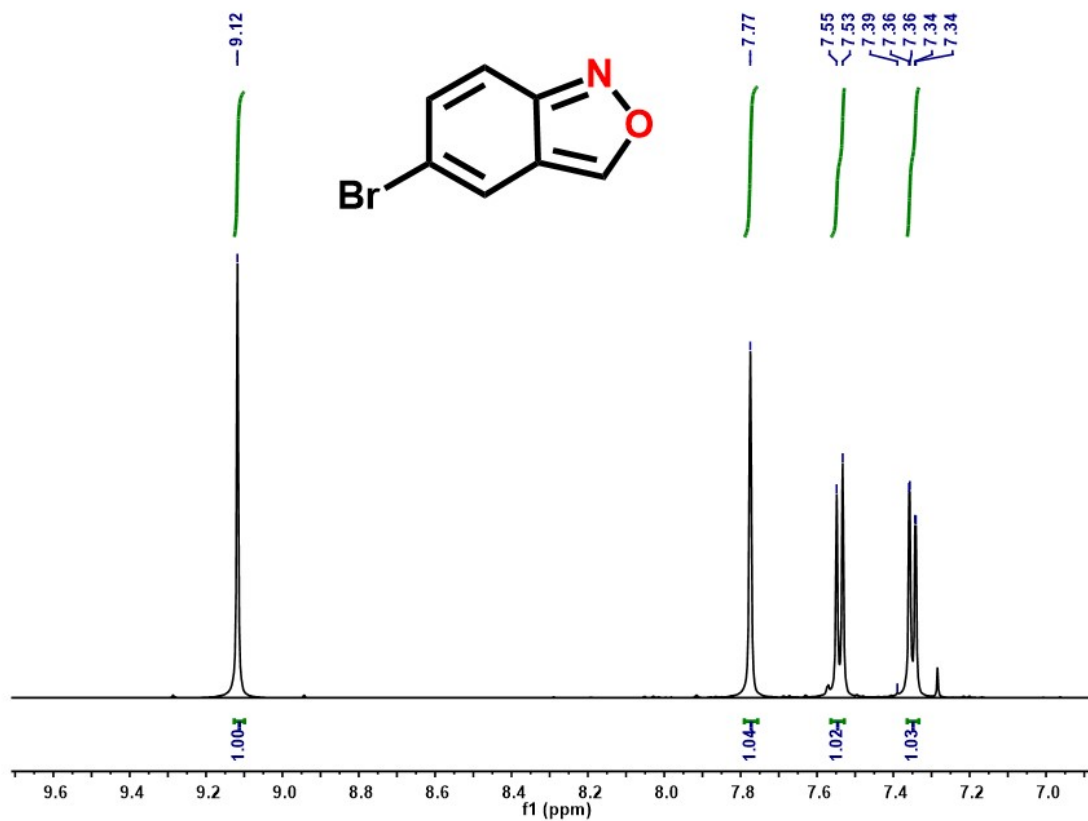
Figure S19 ^{1}H and ^{13}C NMR spectra for 5-bromo-2,1-benzisoxazole.
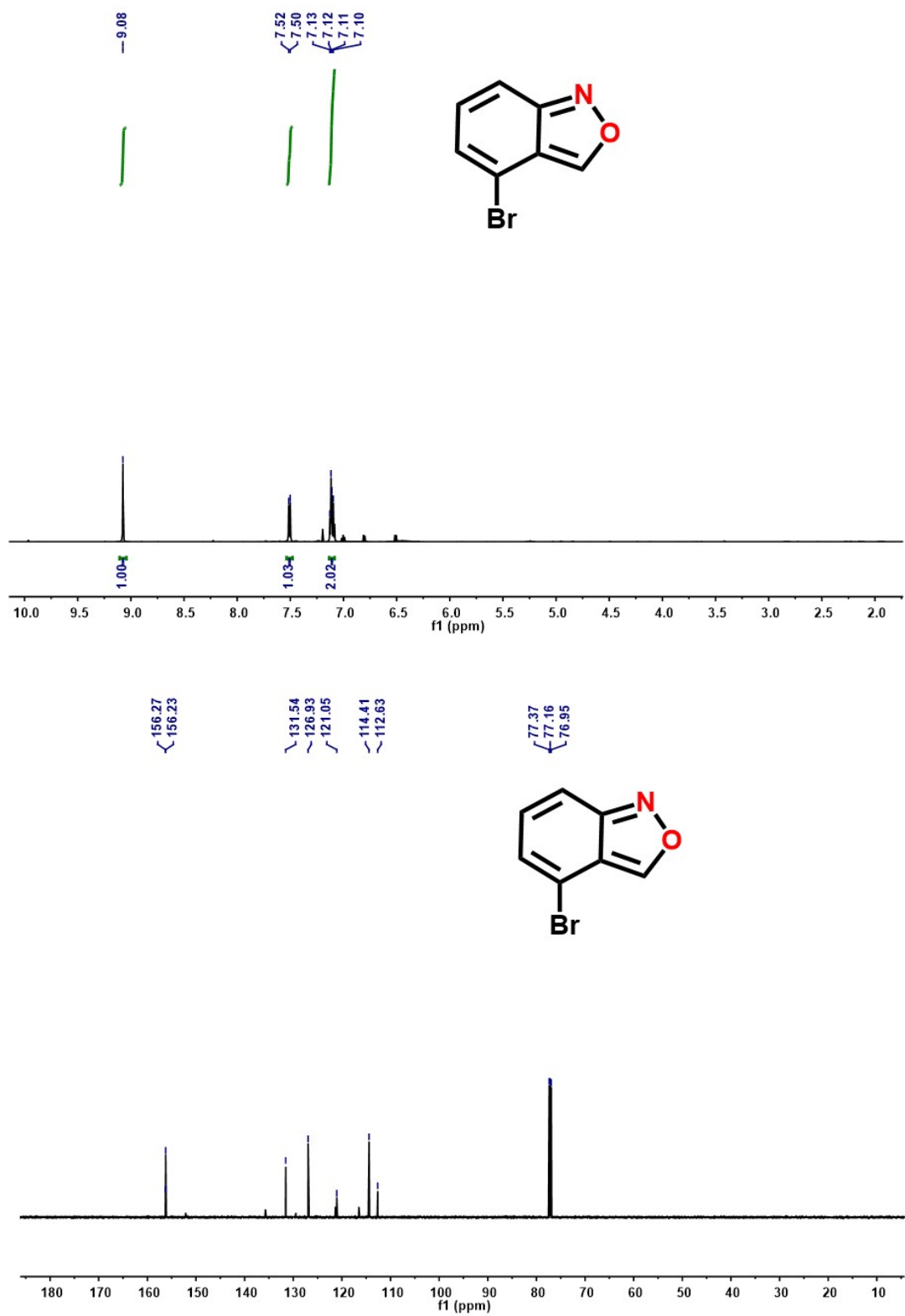
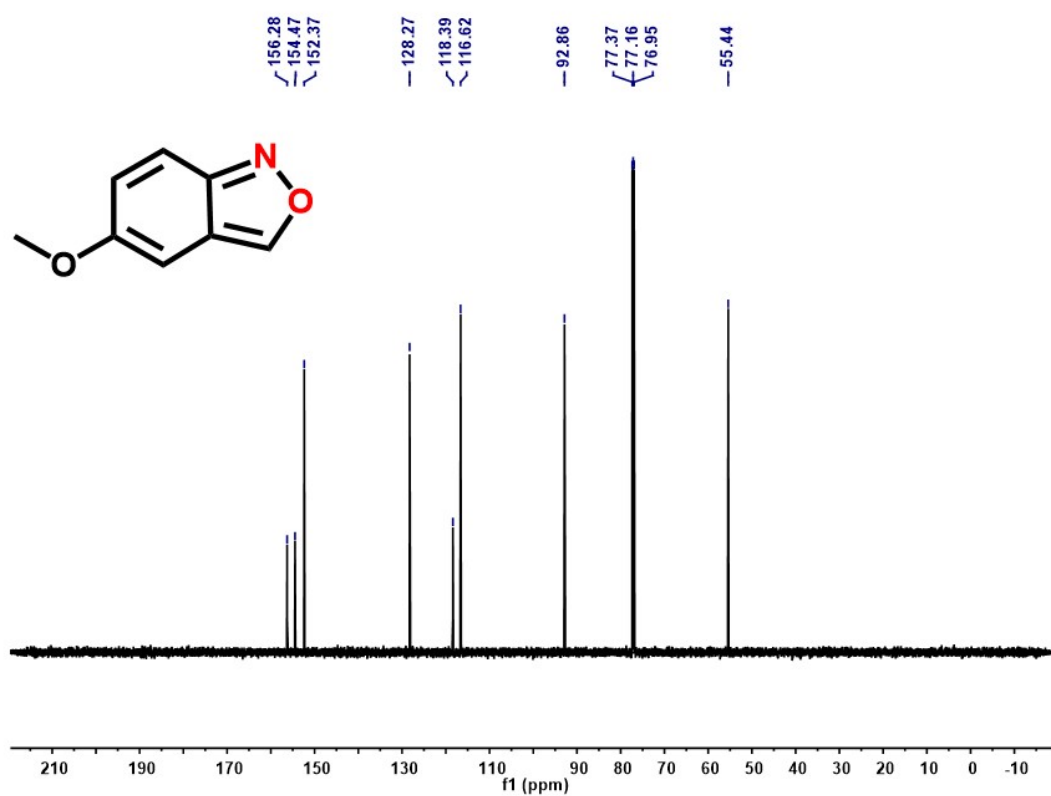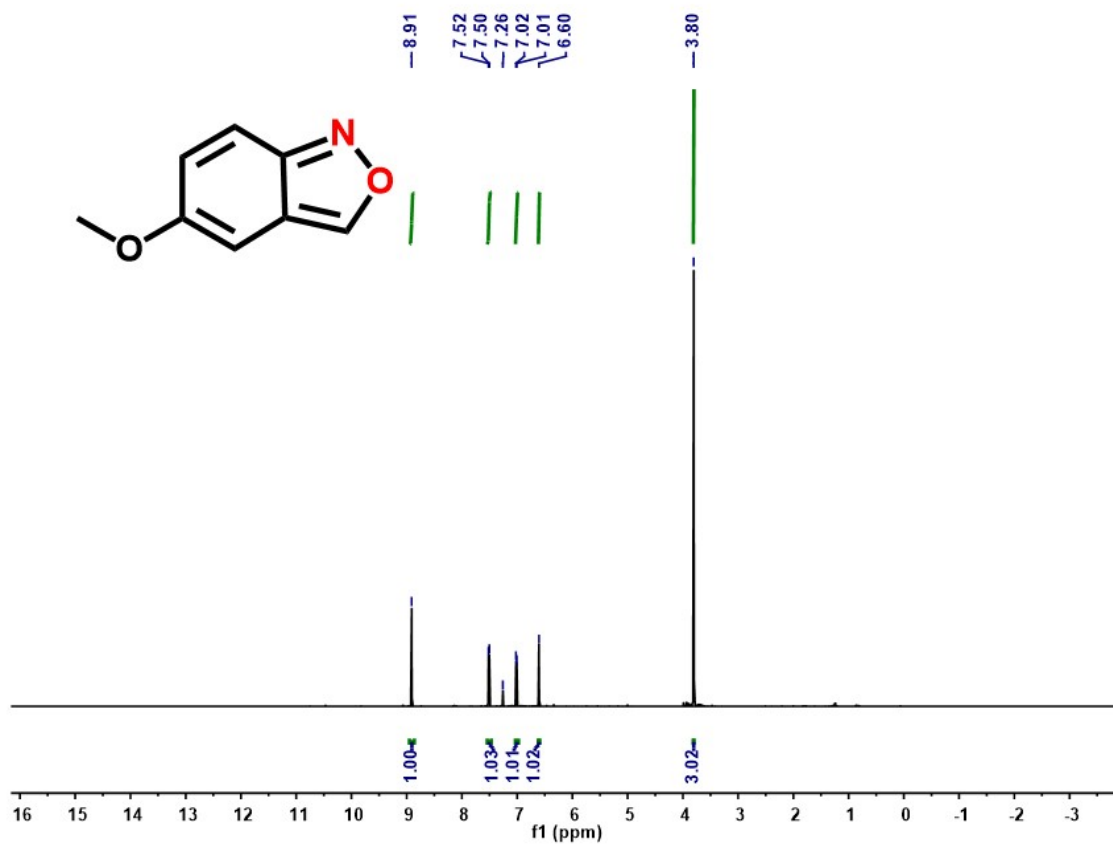**Figure S20** ^{1}H and ^{13}C NMR spectra for 4-bromo-2,1-benzisoxazole.

Figure S21 ^{1}H and ^{13}C NMR spectra for 5-methoxy-2,1-benzisoxazole.

References

[S7]   S. Hosseini, S. A. Bawel, M. S. Mubarak and D. G. Peters, *ChemElectroChem*, 2018, **6**, 4318–4324.

[S8]   H. M. Jin, L. Huang, J. Xie, M. Rudolph, F. Rominger and A. S. K. Hashmi, *Angew. Chem. Int. Ed.*, 2016, **55**, 794–797.

[S9]   P. Raju, G. G. Rajeshwaran, M. Nandakumar and A. K. Mohanakrishnan, *Eur. J. Org. Chem.*, 2015, **2015**, 3513–3523.

[S10]   Q. Cheng, J.-H. Xie, Y.-C. Weng and S.-L. You, *Angew. Chem. Int. Ed.*, 2019, **58**, 5739–5743.

[S11]   R. L. Sahani and R.-S. Liu, *Angew. Chem. Int. Ed.*, 2017*, **56**, 12736–12740.